Electronic Supplementary Information

Catalytic decoloration of methyl orange solution by nanoporous metals

Masataka Hakamada*, Fumi Hirashima, Mamoru Mabuchi

Department of Energy Science and Technology, Graduate School of Energy Science, Kyoto University, Yoshidahonmachi, Sakyo, Kyoto 606-8501, Japan

1. Experimental details

Fabrication of nanoporous Au. A starting $Au_{0.3}Ag_{0.7}$ alloy sheet with thickness of 0.2 mm was fabricated by arc melting, homogenization annealing, cold rolling and cutting. Dealloying of the $Au_{0.3}Ag_{0.7}$ alloy sheet by free corrosion was conducted by immersion of the alloy sheet in 70 mass% HNO_3 at 263 K for 15 h (for Sample 1) and 298 K for 24 h (for Sample 2). Sample 3 was fabricated through electrochemical dealloying using the $Au_{0.3}Ag_{0.7}$ alloy sheet as a working electrode, that is, by electrolysis in 0.1 mol/L HNO_3 for 10 h at a potentiostatic condition of +1.1 V vs. a saturated calomel electrode (SCE) at room temperature.

Fabrication of nanoporous Pd. A starting $Pd_{0.2}Co_{0.8}$ alloy sheet was fabricated by arc melting, homogenization annealing, cold rolling and cutting. Electrolysis using the $Pd_{0.2}Co_{0.8}$ alloy sheet as a working electrode was conducted in 0.1 mol/L H_2SO_4 for 15 h at a potentiostatic condition at +0.5 V vs. SCE at room temperature.

Fabrication of nanoporous Ni. A starting $Ni_{0.3}Mn_{0.7}$ alloy sheet was fabricated by arc melting, homogenization annealing, cold rolling and cutting. Electrolysis using the $Ni_{0.3}Mn_{0.7}$ alloy sheet as a working electrode was conducted in 1 mol/L $(NH4)_2SO_4$ aqueous solution for 10 h at a potentiostatic condition at −0.65 V vs. SCE at room temperature.

Characterization. Samples were observed using a field-emission scanning electron microscope (FE-SEM, SU6600 by Hitachi High-Technology Corp.) equipped with

energy-dispersive X-ray spectroscopy (EDXS). The roughness factor of the nanoporous Au samples, which is the ratio of the electrochemically active surface area of nanoporous Au to that of smooth Au, was estimated using the charge associated with the reduction of adsorbed oxygen during cyclic voltammetry in 0.1 mol/L H_2SO_4 (Trasatti and Petrii, *J. Electroanal Chem.* **327** (1992) 353).

High-performance liquid chromatography (HPLC). Target solutions (10 μL) were analyzed using HPLC. Columns of Shim-pack VP-ODS with length of 150 mm and inner diameter of 4.6 mm were employed. The mobile phase was composed of two components; one is 10 mmol/L sodium phosphate buffer solution (pH 2.6) with 100 mmol/L sodium perchlorate and the other is acetonitrile. Gradient analysis at 313 K with a flow rate of 0.8 mL/min was conducted according to the concentration schedule shown in Table S1.

Table S1. Concentration schedule for HPLC.

Time (min)	Concentration of acetonitrile (%)
0.00	5
10.00	70
15.00	70
15.01	5
22.00	Stop

2. Additional results

Immersion of TiO_2 and ZnO sheets. Figure S1 shows the time variation of methyl orange (MO) concentration after immersion of TiO_2 and ZnO sheets in the MO solution under a dark condition. No decrease in MO concentration was detected. This is due to the absence of light irradiation, because photocatalytic TiO_2 and ZnO require light for decomposition of MO.

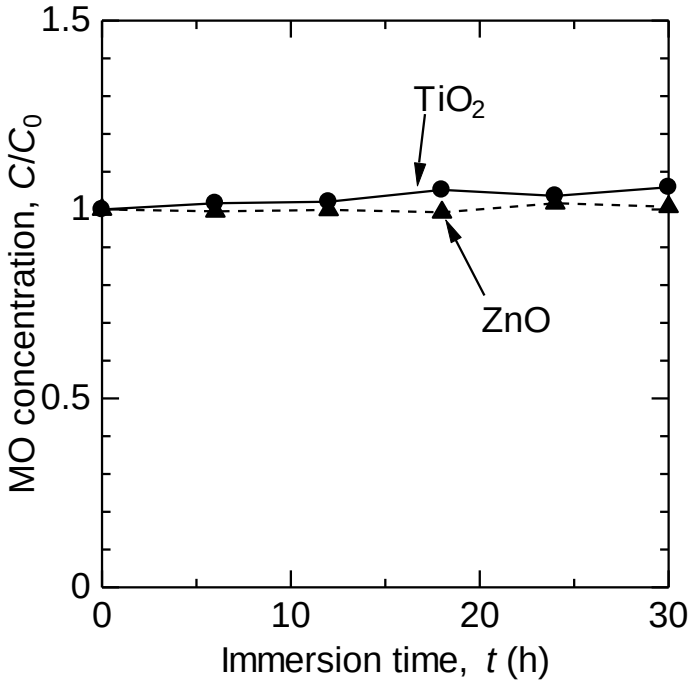

Figure S1. Time variation of methyl orange concentration after the immersion of TiO_2 and ZnO sheets under a dark condition.

Logarithmic decrease in MO concentration by nanoporous Au. Figure S2 shows the logarithmic decrease in MO concentration after the immersion of nanoporous Au samples in the MO solution. The plots are well represented along the straight lines. This suggests that first-order reaction kinetics is reasonable for the MO decomposition.

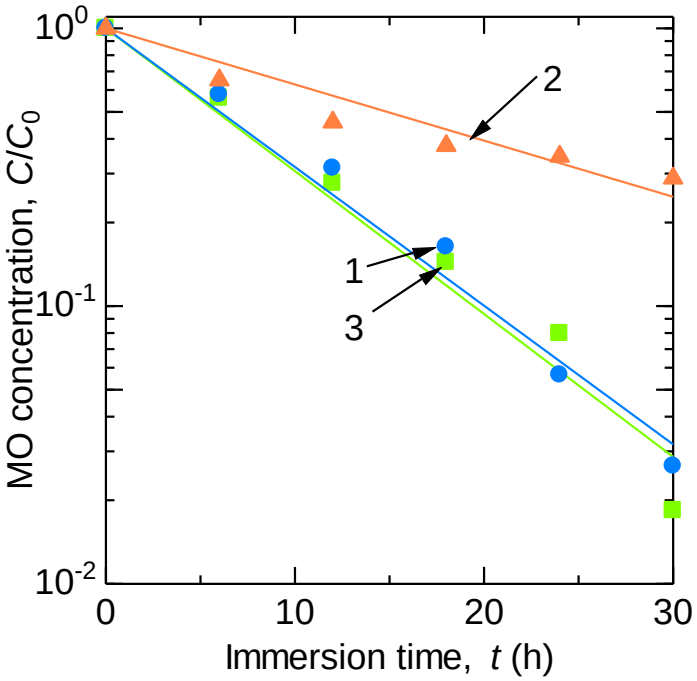

Figure S2. Time variation of MO concentration after the immersion of nanoporous Au samples in the MO solution measured according to a logarithmic scale. The numbers indicate the Sample No. presented in Table 1.

SEM images of nanoporous Pd and Ni. Figure S3 shows the SEM images of nanoporous Pd and Ni. Ligament sizes of 20 and 9 nm were observed in nanoporous Pd and Ni, respectively.

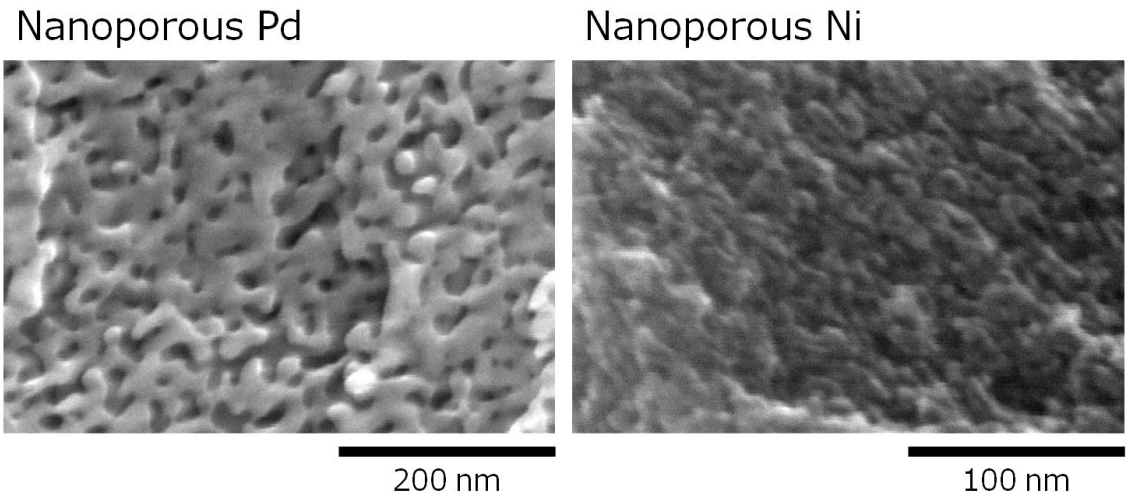

Figure S3. SEM images of nanoporous Pd and Ni.

Immersion of bulk Pd and Ni sheets. Figure S4 shows the MO solution after 120-h immersion of bulk Pd and Ni sheets as well as control run (without sample immersion). Bulk Pd and Ni exhibited no decoloration of MO solution.

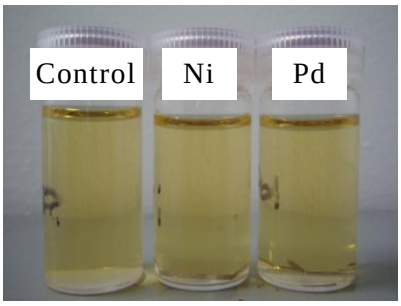

Figure S4. MO solution (initial concentration of 2×10^{-5} mol/L) after 120-h immersion of bulk Pd and Ni sheets. Bulk Pd and Ni exhibited no decoloration on MO solution.

XPS analyses. Figure S5 shows the X-ray photoelectron spectra of nanoporous Au (sample 1) before and after MO decoloration. The Au 4f peaks were not shifted by the decoloration, indicating that Au complex with the dye does not form.

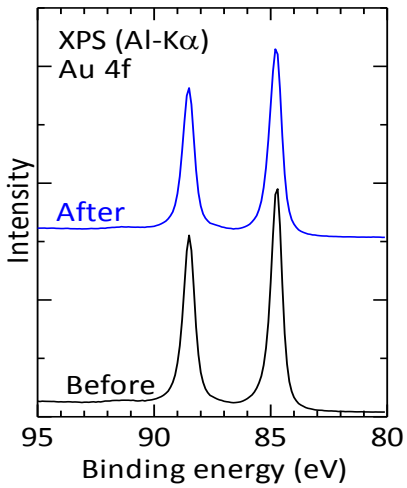

Figure S5. X-ray photoelectron spectra of nanoporous Au (sample 1) before and after MO decoloration.